Magnetic tunnel junctions using B2-ordered Co2MnAl Heusler alloy epitaxial electrode

Magnetic tunnel junctions using *B*2-ordered Co_2MnAl Heusler alloy epitaxial electrode

Y. Sakuraba,[a] J. Nakata, M. Oogane, Y. Ando, H. Kato, A. Sakuma, and T. Miyazaki
Department of Applied Physics, Graduate School of Engineering, Tohoku University, Aoba-yama 6-6-05, Aramaki, Aoba-ku, Sendai 980-8579, Japan

H. Kubota
Nanoelectronics Research Institute, National Institute of Advanced Industrial Science and Technology (AIST), 1-1-1 Umezono, Tsukuba 305-8568, Japan

(Received 25 September 2005; accepted 25 November 2005; published online 9 January 2006)

Magnetic tunnel junctions were fabricated with epitaxially grown Co_2MnAl bottom electrodes combined with an Al–O tunnel barrier using a magnetron sputtering system. The epitaxial Co_2MnAl electrode had very low surface roughness of 0.2 nm and a highly ordered *B*2 structure. Magnetic tunnel junctions (MTJs) with a stacking structure of epitaxial-Co_2MnAl/Al–O/CoFe/IrMn exhibited large tunnel magnetoresistance (TMR) ratios of 65% at room temperature and 83% at 10 K. The TMR ratios were larger than those of a MTJ with a Co_2MnAl polycrystalline electrode. © *2006 American Institute of Physics*. [DOI: 10.1063/1.2162867]

Half-metallic ferromagnets (HMFs), which have only one spin-band electron at Fermi energy, have promising potential for application to spintronics device such as magnetic tunnel junctions (MTJs) and spin polarizers for current injection into semiconductors as electrodes. Recently, some groups of full-Heusler alloy X_2YZ compounds (Co_2MnSi, Co_2MnGe, Co_2CrAl, etc.) have attracted much interest because of their predicted half-metallic band structure and high Curie temperatures.[1–3] According to Julliere's model, MTJs using HMFs as both electrodes have extraordinarily large magnetoresistance (MR) ratios.[4]

Full-Heusler alloys belong to a group of ternary intermetallic compounds of general formula X_2YZ formula with a $L2_1$ structure. Full-Heusler alloys also have *B*2 and *A*2 structures depending on their site-disordered state, in which (Y,Z) and (X,Y,Z) are randomly substituted, respectively. According to theoretical calculations, the spin polarization of $L2_1$-ordered full-Heusler alloy is very sensitive to site disordering because the upper and lower edge states of the minority band gap are derived from localized antibonding states on the Co site.[2] Picozzi *et al.* also indicated, using *ab initio* full potential linearized augmented plane wave calculations, that spin polarization of Co_2MnSi and Co_2MnGe was decreased greatly by Co antisites because of a defect-induced in-gap state for the minority spin band.[5] Recently, we have successfully produced a highly $L2_1$-ordered Co_2MnSi epitaxial film by optimizing fabrication conditions and applied it to a bottom electrode of MTJ.[6] An observed MR ratio of 159% at 2 K and estimated spin polarization of 0.89 are the largest values reported for MTJs with an Al–O amorphous barrier. However, its spin polarization was less than 1, indicating that some *B*2-type or *A*2-type site disorders exist in our Co_2MnSi electrode. Actually, site disorder and defects have been observed, even in well-prepared full-Heusler alloys.[7,8] A neutron diffraction experiment conducted by Raphael *et al.* revealed the existence of 10%–14% antisite disorder between Co and Mn sites in the Co_2MnSi bulk sample. For that reason, it is difficult to fabricate $L2_1$-ordered full-Heusler alloy films with no structural imperfections. In addition, heating to high temperatures (400–600 °C) is necessary for full-Heusler alloys to form a highly ordered $L2_1$-structure, but these heating processes over 400 °C for top electrodes are generally undesired because of the problem of heat endurance in MTJs. From these perspectives, Co_2MnAl is an attractive compound because large spin polarization of 0.76 is expected even in a *B*2 structure that can be obtained easily through heating at lower temperatures (200–300 °C).[9] Experimentally, MTJs were fabricated with a polycrystalline Co_2MnAl bottom electrode having *B*2 structure. We showed TMR ratios of 40% at RT and 65% at low temperature (10 K).[9] However, the values were comparable to those of MTJs with conventional ferromagnets such as Co–Fe or Ni–Fe. The present study employs the potential of Co_2MnAl as a MTJ electrode by optimizing the surface roughness and crystal structure of Co_2MnAl.

All samples were grown using inductively coupled plasma-assisted magnetron sputtering. The Co_2MnAl (100) epitaxial bottom electrode was deposited on the Cr-buffered MgO (100) substrate at ambient temperature and postannealed at 300 °C to improve the site-ordered state. Detailed descriptions of bottom-electrode fabrication processes have been reported elsewhere.[10] Crystallographic structures and surface morphologies of the Co_2MnAl were investigated using x-ray diffraction (XRD) and atomic force microscopy (AFM). Magnetization was measured using a superconducting quantum interference device (SQUID). The prepared MTJs had the following stacking structure: MgO (100)/epitaxial Cr 40 nm/epitaxial Co_2MnAl 30 nm/Al–O 1.3 nm/$Co_{75}Fe_{25}$ 5 nm/$Ir_{22}Mn_{78}$ 10 nm/Ta 5 nm/. The Al–O tunneling barrier layer was prepared using plasma oxidation with optimized oxidation times t_{ox} between 60 and 300 s. The MTJs were patterned into 10×10 μm^2–100×100 μm^2 using microfabrication processes including Ar ion etching and CHF_3 reactive ion etching. The MTJs were annealed in high vacuum by applying a 300 Oe magnetic field. Magnetoresistance curves were measured using standard four-probe method between 4.2 K and RT.

[a]Electronic mail: sakuraba@mlab.apph.tohoku.ac.jp

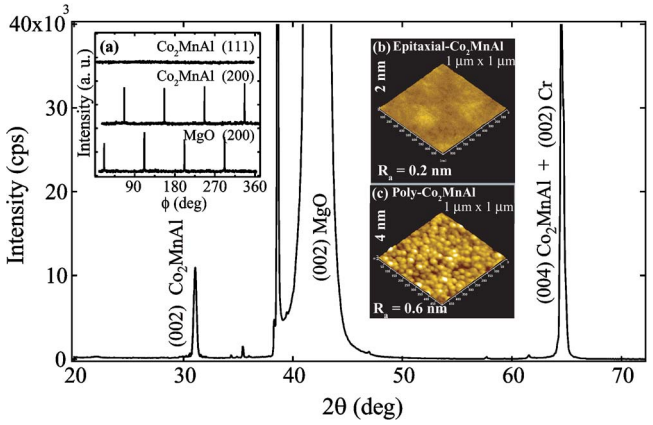

FIG. 1. (Color online) XRD (θ–2θ scan) pattern of MgO/Cr (40 nm)/Co_2MnAl (30 nm) film. Inset (a) shows ϕ scans of (200) plane for the MgO substrate and (200) and (111) planes for Co_2MnAl film. Insets (b) and (c), respectively, show surface morphology images of epitaxial and 50-nm-thick polycrystalline Co_2MnAl films.

The Co_2MnAl bottom electrode's XRD pattern is shown in Fig. 1. Only the (002) Cr peak and the (002) and (004) Co_2MnAl peaks were observed, indicating perfect (001)-oriented growth in the direction perpendicular to the film plane. The ϕ scan of (200) planes of MgO substrate and Co_2MnAl film revealed epitaxial growth of Co_2MnAl films with in-plane relation of MgO[011]/Co_2MnAl[001], as shown in inset (a). In these XRD measurements, clear (200) peaks derived from $B2$-type superlattice were observed, but a (111) peak from $L2_1$-type superlattice was not detected in Co_2MnAl. Therefore, the fabricated epitaxial Co_2MnAl was identified as a highly ordered $B2$ structure, not an $L2_1$ structure. The AFM images of the epitaxial and polycrystalline Co_2MnAl are shown, respectively, in insets (b) and (c). Extremely flat surface morphology was observed in the epitaxial Co_2MnAl surface. The estimated average surface roughness R_a of 0.2 nm was much less than that of the polycrystalline Co_2MnAl (~0.6 nm) that was examined in our previous study.[9] In addition, the saturation magnetization of Co_2MnAl measured using SQUID is about 4 μ_B/f.u., which is a very important result to obtain high spin-polarization because a half-metallic band structure leads to the integer Bohr magnetron, as indicated by Galanakis *et al.*[2]

Figure 2 shows typical MR curves for MTJs using epitaxial Co_2MnAl measured at 10 and 300 K. Observed MR ratios of 61% at 300 K and 83% at 2 K were large in MTJs using an Al–O amorphous tunneling barrier. The temperature dependence of the MR ratio is plotted in the inset of Fig. 2. Previous results obtained for MTJs with polycrystalline Co_2MnAl and $Co_{75}Fe_{25}$ are also shown for comparison.[9,11] The MTJ with epitaxial Co_2MnAl shows the largest MR ratio in all temperature ranges. In addition, the spin polarization of epitaxial Co_2MnAl estimated from Julliere's equation was 0.59 (assuming 0.50 for $Co_{75}Fe_{25}$).

The MR ratios and resistance area products ($R \times A$) for epitaxial-Co_2MnAl/Al–O/$Co_{75}Fe_{25}$ (MTJ-1) are plotted in Fig. 3 as a function of t_{ox}. Results of normal $Co_{75}Fe_{25}$/Al–O/$Co_{75}Fe_{25}$ junctions (MTJ-2) that were fabricated using the same sputtering device are also shown for reference. As shown in Fig. 3(a), the $R \times A$ values of MTJ-1 are about two orders of magnitude larger than that of MTJ-2 for all t_{ox} ranges, despite having the same oxidation conditions of the tunnel barrier layer. This enlargement of $R \times A$

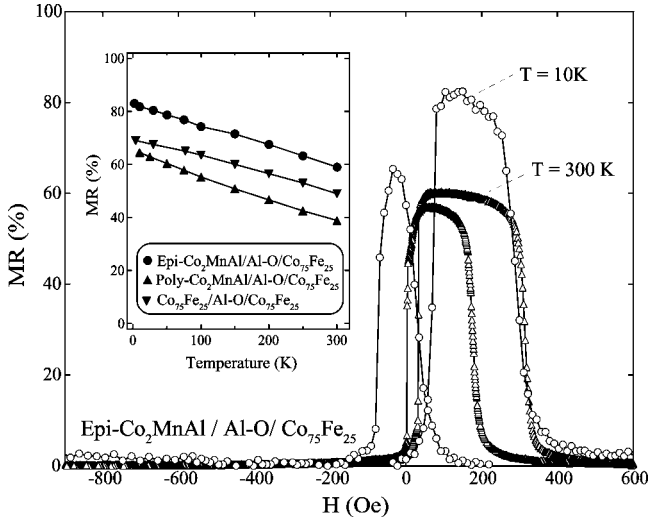

FIG. 2. MR curves of MTJs with the epitaxial Co_2MnAl bottom electrode measured at 10 K (circles) and 300 K (triangles). The oxidation time of Al–O was 130 s. The inset shows the temperature dependence of MR ratios for MTJs using epitaxial Co_2MnAl, polycrystalline Co_2MnAl, and $Co_{75}Fe_{25}$.

values was similar to that found for MTJs with the Co_2MnSi bottom electrode in a previous study.[6,12] Another result is noteworthy: MR ratios of MTJ-1 increased slightly to 65% with increasing t_{ox}, in contrast to the drastic decrease of MTJ-2. High-resolution cross-sectional transmission electron microscopy (TEM) images of semiepitaxial MTJs that were fabricated in the present study and those of polycrystalline

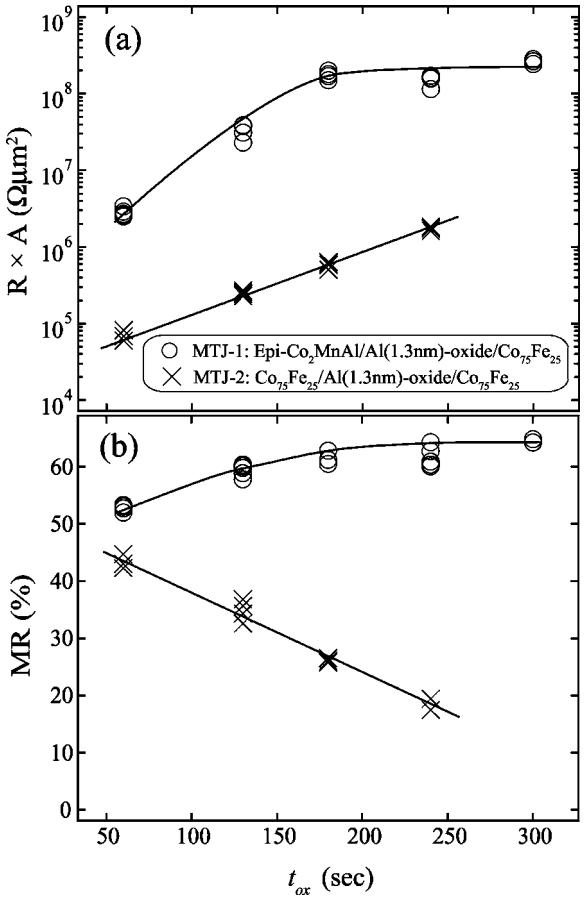

FIG. 3. Oxidation time dependence of resistance area products (a) and MR ratios (b) of MTJ with Co_2MnAl bottom electrode (MTJ-1) and CoFe bottom electrode (MTJ-2).

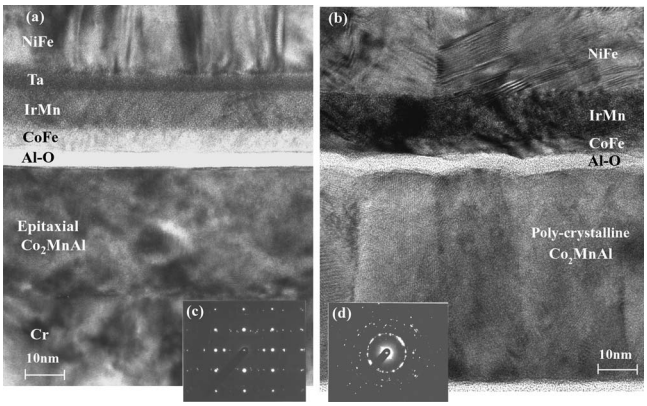

FIG. 4. Cross-sectional TEM images of MTJs with epitaxial Co_2MnAl bottom electrode (a) and polycrystalline electrode (b). Electron diffraction patterns of respective samples are shown in (c) and (d).

MTJs of a previous study[9] are shown, respectively, in Figs. 4(a) and 4(b). The t_{ox} was 180 s for both samples. Comparison of the two images reveals that the interface flatness between the Al–O barrier layer and Co_2MnAl bottom electrode is improved greatly by epitaxial growth of the bottom electrode. In contrast to the columnar grain growth of polycrystalline Co_2MnAl, single crystalline growth was confirmed in epitaxial Co_2MnAl. Electron diffraction patterns (c) and (d) also show good structural quality and perfect (001)-oriented growth of epitaxial Co_2MnAl. The large MR ratio is attributable to these improvements of the interface and structural quality of Co_2MnAl. An interesting point is that the estimated thickness of the amorphous barrier layer, denoted as "Al–O" in the TEM image, was about 3–4 nm, which is 2–3 times larger than the deposited Al layer thickness of 1.3 nm. This thicker barrier layer is inferred to be related to enlargement of the $R \times A$ value shown in Fig. 3(a).

Schmalhorst *et al.* studied the interface structure and magnetism of MTJs with Co_2MnSi using x-ray absorption spectroscopy (XAS) and x-ray circular dichroism.[12] They noted that the plasma-oxidation process of the Al-oxide barrier layer induced Mn/Si segregation and oxide formation at the lower barrier interface. The MR ratios decreased greatly, especially at room temperature, as a result of the spin-independent tunneling path resulting from interface impurities. Our previous study also showed a large decrease of MR ratios in the Co_2MnSi MTJs with an overoxidized Al–O barrier layer.[6] Oxidation of the bottom Co_2MnAl electrode must have occurred in the present study, as indicated by TEM images and large $R \times A$ values. It is very interesting, however, that MR ratios remain large despite the overoxidation of the bottom electrode surface in Fig. 3(b). This unique phenomenon remains unexplained, but we have inferred that the interface impurity of the Co_2MnAl electrode does not increase the spin scattering of tunneling electrons greatly in comparison to that of Co_2MnSi electrode. Further observations of interface magnetic impurities using XAS or inelastic tunneling spectroscopy are necessary to clarify this difference.

In summary, this study fabricated magnetic tunnel junctions with a (100)-epitaxial Co_2MnAl bottom electrode and Al–O insulating tunnel barrier. The epitaxial Co_2MnAl bottom electrode showed very low surface-roughness ($\sim$0.2 nm) and highly ordered $B2$ structure. The plasma oxidation process of the Al–O tunnel barrier caused rapid oxidation of the bottom Co_2MnAl surface because Co_2MnAl has very easily oxidized atoms as constituents: Mn and Al. Oxidation of the bottom electrode interface increased the $R \times A$ value, but did not decrease the MR ratio. The obtained maximal MR ratio of 65% at room temperature and 83% at 2 K was large in MTJs with an amorphous tunneling barrier. This result suggested that Co_2MnAl is a highly spin-polarized material, as predicted by theoretical calculations. However, the estimated spin-polarization value of 0.59 by Julliere's equation was still smaller than the expected value of 0.76 for the $B2$ structure.[9] Further optimizations of Co_2MnAl electrode (e.g., adjustment of compositional deviation from stoichiometry) engender ideal spin polarization and enhanced MR ratios.

The authors are grateful to Dr. S. Yuasa of the National Institute of Advanced Industrial Science and Technology (AIST) for helpful discussion related to this study. This study was supported by the IT-Program of the Research Revolution 2002 (RR2002) "Development of Universal Low-Power Spin Memory" and a Grant-in-Aid for Scientific Research from the Ministry of Education, Culture, Sports, Science and Technology of Japan, CREST of Japan Science and Technology (JST), the NEDO Grant Program, and JSPS Research Fellowships for Young Scientists.

[1] S. Ishida, S. Fujii, S. Kashiwagi, and S. Asano, J. Phys. Soc. Jpn. **64**, 2152 (1995).
[2] I. Galanakis, P. H. Dederiches, and N. Papanikolaou, Phys. Rev. B **66**, 174429 (2002).
[3] S. Picozzi, A. Continenza, and A. J. Freeman, Phys. Rev. B **66**, 094421 (2002).
[4] M. Julliere, Phys. Lett. **54A**, 225 (1975).
[5] S. Picozzi, A. Continenza, and A. J. Freeman, Phys. Rev. B **69**, 094423 (2004).
[6] Y. Sakuraba, J. Nakata, M. Oogane, H. Kubota, Y. Ando, A. Sakuma, and T. Miyazaki, Jpn. J. Appl. Phys., Part 2 **44**, L1100 (2005).
[7] B. Ravel, M. P. Raphael, Q. Huang, and V. G. Harris, Phys. Rev. B **65**, 184431 (2002).
[8] S. B. Ravel, J. O. Cross, M. P. Raphael, V. G. Harris, R. Ramesh, and V. Saraf, Appl. Phys. Lett. **81**, 2812 (2002).
[9] H. Kubota, J. Nakata, M. Oogane, Y. Ando, A. Sakuma, and T. Miyazaki, Jpn. J. Appl. Phys., Part 2 **43**, L984 (2004).
[10] Y. Sakuraba, J. Nakata, M. Oogane, H. Kubota, Y. Ando, A. Sakuma, and T. Miyazaki, Jpn. J. Appl. Phys., Part 1 **44**, 6535 (2005).
[11] X.-F. Han, M. Oogane, H. Kubota, Y. Ando, and T. Miyazaki, Appl. Phys. Lett. **77**, 283 (2000).
[12] J. Schmalhorst, S. Kämmerer, M. Sacher, A. Hütten, G. Reiss, and A. Scholl, Appl. Phys. Lett. **85**, 79 (2004).